Role of projectile breakup effects and intrinsic degrees of freedom on fusion dynamics *

Manjeet Singh Gautam[1)]

Department of Physics, Indus Degree College, Kinana, Jind-126102 (Hargana), India

Abstract: This article analyzes the fusion dynamics of loosely bound and stable projectiles with Zr-target isotopes within the context of the coupled channel approach and the energy-dependent Woods-Saxon potential model (EDWSP model). In the case of the ^{28}Si+^{90}Zr reaction, the coupling to the inelastic surface excitations results in an adequate description of the observed fusion dynamics while in case of the ^{28}Si + ^{94}Zr reaction, the coupling to collective surface vibrational states as well as the neutron (multi-neutron) transfer channel is necessary in the coupled channel calculations to reproduce the below-barrier fusion data. However, the EDWSP model calculation provides an accurate explanation of the fusion data of ^{28}Si + ^{90,94}Zr reactions in the domain of the Coulomb barrier. In the fusion of the ^{6}Li + ^{90}Zr reaction, the inclusion of the nuclear structure degrees of freedom recovers the observed sub-barrier fusion enhancement but results in suppression of the above barrier fusion data by 34% with respect to the coupled channel calculations. Using EDWSP model calculations, this suppression factor is reduced by 14% and consequently, the above-barrier fusion data of ^{6}Li+^{90}Zr reaction is suppressed by 20% with reference to the EDWSP model calculations. Such fusion suppression at above-barrier energies can be correlated with the breakup of the projectile (^{6}Li) before reaching the fusion barrier, as a consequence of low binding energy.

Keywords: heavy-ion sub-barrier fusion reactions, coupled channel equations, weakly bound nuclei

PACS: 25.60.Pj, 21.60.Ev, 24.10.Eq **DOI:** 10.1088/1674-1137/40/5/054101

1 Introduction

The advancement of radioactive beams has increased interest in exploration of the fusion dynamics of colliding systems involving loosely bound nuclei and/or halo nuclei at near and sub-barrier energies. The various interesting features of heavy fusion reactions like fusion enhancement and fusion suppression are associated with the nuclear structure of participating nuclei. It has been recognized that the fusion mechanism of tightly bound nuclei in the close vicinity of the Coulomb barrier is strongly influenced by the intrinsic structure degrees of freedom of the colliding pairs [1–7]. For stable nuclei, the coupling of the relative motion of the colliding nuclei to their nuclear structure degrees of freedom, like collective surface vibrational states (spherical nuclei), rotational states (deformed nuclei), nucleon (multi-nucleon) transfer channels etc., eliminates the discrepancies between experimental fusion data and the expectations of the one-dimensional barrier penetration model [8–13]. However, in the fusion of colliding systems involving weakly bound nuclei (or halo nuclei), the breakup channel significantly affects the fusion process in the close vicinity of the Coulomb barrier [14,15]. Several theoretical investigations have suggested that the fusion excitation functions are suppressed because of breakup effects [16–18] while some other theoretical studies give indications of the enhancement of fusion cross-sections due to breakup effects in the domain of the Coulomb barrier [19, 20]. For instance, in the case of ^{38}S + ^{181}Ta [21], ^{6}He + ^{209}Bi [22, 23] and ^{6}He + ^{238}U reactions [24], there is enhancement of the fusion excitation function data, while in the fusion of ^{9}Be+^{208}Pb [25],^{9}Be+^{209}Bi [26], ^{6,7}Li+^{209}Bi [27] and ^{6}Li+^{144}Sm reactions [28], there is suppression of the above-barrier fusion data with reference to theoretical predictions. In the fusion of the ^{7}Li+^{165}Ho reaction, the reduction of above-barrier fusion excitation function data and the fusion enhancement at below-barrier energies has been pointed out [29]. Therefore, the enhancement or suppression of fusion cross-section due to breakup effects is still open and more extensive studies are required to obtain a definite conclusion.

The fusion of the ^{6}Li+^{90}Zr reaction was recently measured using the off-line γ-ray spectroscopy method and

Received 9 July 2015

∗ Supported by Dr. D. S. Kothari Post-Doctoral Fellowship Scheme sponsored by University Grants Commission (UGC), New Delhi, India

1) E-mail: gautammanjeet@gmail.com

the authors have shown that the above-barrier fusion excitation function data is suppressed by a factor of 34% with respect to the coupled channel calculations [30]. The fusion dynamics of the ^{6}Li + ^{90}Zr reaction is quite interesting because the projectile is a loosely bound nucleus due to its low breakup threshold (B.E. = 1.475 MeV). Using the continuum discretized coupled channel (CDCC) approach, the authors clearly identified the role of the breakup channel and suggested that the above-barrier suppression occurs as a result of projectile breakup effects [31, 32]. Following this, the present work provides a theoretical description of the fusion dynamics of the ^{6}Li + ^{90}Zr reaction within the view of the EDWSP model [33, 34] and coupled channel approach [35]. To ensure the suppression of the ^{6}Li + ^{90}Zr reaction at above-barrier energies, the fusion dynamics of ^{28}Si + ^{90,94}Zr reactions, wherein the projectile (^{28}Si) is stable against breakup effects, has been included in the present article [36–38]. The target isotopes (^{90,94}Zr) are spherical in shape and exhibit low lying inelastic surface vibrational states as the dominant mode of couplings. The fusion dynamics of ^{28}Si+^{90,94}Zr reactions is expected to behave in a similar way to that of ^{32,36}S + ^{90,96}Zr and ^{40,48}Ca + ^{90,96}Zr reactions [39, 40] wherein the role of multi-neutron transfer channels have been precisely identified. In the fusion of the ^{28}Si+^{90}Zr reaction, the inclusion of the collective surface vibrational states of fusing systems produces substantially large sub-barrier fusion enhancement over the expectations of the one dimensional barrier penetration model [36–38]. However, in the case of the ^{28}Si + ^{94}Zr reaction, the couplings to inelastic surface excitations of the colliding pairs as well as the neutron (multi-neutron) transfer channels are required to achieve a complete description of the sub-barrier fusion enhancement. The common target isotope (^{90}Zr) participates equally in ^{6}Li+^{90}Zr and ^{28}Si+^{90}Zr reactions and a comparison of the above-barrier fusion data of these reactions shows the influence of the projectile breakup channel on the fusion process. The coupled channel calculations and the EDWSP model calculations reasonably explain the observed fusion dynamics of ^{28}Si+^{90,94}Zr reactions. In the case of the ^{6}Li+^{90}Zr reaction, the above-barrier fusion data is suppressed by 34% with reference to the coupled channel calculations [30]. Interestingly, this suppression is minimized by about 14% and consequently, the experimental data of ^{6}Li + ^{90}Zr reaction at above-barrier energies is suppressed by 20% with reference to the EDWSP model calculations. For all three reactions, the discrepancies between expectations of the one-dimensional barrier penetration model and experimental data can be removed if one either entertains the effects of nuclear structure degrees of freedom in the coupled channel model or makes use of the EDWSP model along with the one-dimensional Wong formula [41]. A brief description of the method of calculation is given in Section 2. The results are discussed in Section 3 and the conclusions drawn are described in Section 4.

2 Theoretical formalism

2.1 Single channel description

The total fusion cross-section is defined as

$$\sigma_{\rm F} = \frac{\pi}{k^2}\sum_{\ell=0}^{\infty}(2\ell+1)T_{\ell}^{\rm F}. \tag{1}$$

Based on the parabolic approximation, Hill and Wheeler proposed an expression for tunneling probability ($T_{\ell}^{\rm F}$) wherein the effective interaction between the collision partners is replaced by an inverted parabola [42]

$$T_{\ell}^{\rm HW} = \frac{1}{1+\exp\left[\dfrac{2\pi}{\hbar\omega_{\ell}}(V_{\ell}-E)\right]}. \tag{2}$$

Following Wong's assumptions in the above expression and by taking the effects of the infinite number of partial waves, one can obtain the following expression of the one dimensional Wong formula [41].

$$\sigma_{\rm F} = \frac{\hbar\omega R_{\rm B}^2}{2E}\ln\left[1+\exp\left(\frac{2\pi}{\hbar\omega}(E-V_{\rm B})\right)\right]. \tag{3}$$

Recently, it has been explicitly shown that the EDWSP model is an effective theoretical approach to explore fusion dynamics [33, 34]. The fusion of spherical colliding nuclei, where either nucleon (multi-nucleon) transfer channels or inelastic surface excitations or both are dominant mode of couplings, has been successfully probed using the EDWSP model. In this work, the EDWSP model is used along with the one-dimensional Wong formula and the static Woods-Saxon potential has been used in the coupled channel calculations for theoretical predictions of the fusion excitation functions of weakly bound and stable colliding systems. Therefore, the form of the static Woods-Saxon potential is defined as

$$V_{\rm N}(r) = \frac{-V_0}{\left[1+\exp\left(\dfrac{r-R_0}{a}\right)\right]}, \tag{4}$$

with $R_0 = r_0(A_{\rm P}^{\frac{1}{3}} + A_{\rm T}^{\frac{1}{3}})$. The quantity V_0 is depth and a is the diffuseness parameter of the nuclear potential. In the EDWSP model, V_0 is defined as

$$V_0 = \left[A_{\rm P}^{\frac{2}{3}} + A_{\rm T}^{\frac{2}{3}} - (A_{\rm P}+A_{\rm T})^{\frac{2}{3}}\right] \times \left[2.38 + 6.8\,(1+I_{\rm P}+I_{\rm T})\,\frac{A_{\rm P}^{\frac{1}{3}}A_{\rm T}^{\frac{1}{3}}}{\left(A_{\rm P}^{\frac{1}{3}}+A_{\rm T}^{\frac{1}{3}}\right)}\right] \text{ MeV}, \tag{5}$$

where $I_{\rm P}=\left(\frac{N_{\rm P}-Z_{\rm P}}{A_{\rm P}}\right)$ and $I_{\rm T}=\left(\frac{N_{\rm T}-Z_{\rm T}}{A_{\rm T}}\right)$ are the isospin asymmetry of projectile and target nuclei respectively. In heavy ion fusion reactions, the different kinds of static and dynamical physical effects such as variations of N/Z ratio, variations of surface energy and surface diffuseness of the colliding pairs, variations of nucleon densities in the neck region, dissipation of kinetic energy of relative motion to internal structure degrees of freedom of the colliding nuclei and nuclear structure effects occur in the surface region of nuclear potential and consequently modify the parameters of the static Woods-Saxon potential. The surface region of the nuclear potential is more sensitive to small changes in nucleon density parameters than the inner region, and the nuclear structure effects of colliding nuclei are mostly present at the surface region, and are mainly related to the diffuseness parameter of the nuclear potential. Therefore, due to nuclear structure effects, the strengths of nuclear potential may vary significantly at the surface region, which can be accommodated by varying the diffuseness parameter of the nuclear potential. In addition, the energy dependence in the nucleus-nucleus potential originates from non-local quantum effects [43]. In a recent analysis, it has been explicitly shown that as a consequence of the channel coupling effects, the nucleus-nucleus potential becomes energy dependent in the domain of the Coulomb barrier [44]. Therefore, all such static and dynamical physical effects are included in the present model by considering the energy dependence in the Woods-Saxon potential via its diffuseness parameter. In the EDWSP model, the energy dependent diffuseness parameter is defined as

$$a(E)=0.85\left[1+\frac{r_0}{13.75\left(A_{\rm P}^{-\frac{1}{3}}+A_{\rm T}^{-\frac{1}{3}}\right)\left(1+\exp\left(\frac{\frac{E}{V_{\rm B0}}-0.96}{0.03}\right)\right)}\right]\ {\rm fm}. \tag{6}$$

In the above expression, the range parameter (r_0) is an adjustable parameter and its value is optimized in order to vary the diffuseness parameter required for addressing the observed fusion dynamics of the fusing system under consideration. The value of the range parameter strongly depends on the nature of the colliding system and on the nature of dominance of the nuclear structure degrees of freedom like collective excitations of vibrational states, static deformation, nucleon (multi-nucleon) transfer channels etc. Since all three potential parameters (r_0, a and V_0) are interrelated, variation in one parameter automatically brings corresponding modifications in the values of the other parameters. In our model, the value of V_0 depends on the surface energy and isospin term of the colliding pairs while the other two parameters (r_0 and a) are related through Eq. (6). The variation of the diffuseness parameter is controlled via the range parameter (r_0) that define the radius of colliding systems ($R_0=r_0(A_{\rm P}^{\frac{1}{3}}+A_{\rm T}^{\frac{1}{3}})$). This consistency of radius parameter is also evident from the various coupled channel formulations. In the coupled channel approach, this radius parameter $\{R_0=r_0(A_{\rm P}^{\frac{1}{3}}+A_{\rm T}^{\frac{1}{3}})\}$ is used in the Woods-Saxon potential and the impacts of the intrinsic degrees of freedom of the colliding pairs are incorporated through the radius parameter [35, 45]. The values of range parameters used in the EDWSP model calculations are consistent with the commonly adopted values of the range parameter ($r_0=0.90$ fm to $r_0=1.35$ fm) which are generally used in the literature within the context of the different theoretical models for different projectile-target systems [5, 6, 45, 46].

2.2 Coupled channel description

In this section, a brief description of the coupled channel approach used for the theoretical calculations of the fusion excitation function is presented. In the coupled channel model, the intrinsic degrees of freedom of the colliding pairs like inelastic surface excitations, static deformation and nucleon (multi-nucleon) transfer channels are coupled with the relative motion of the colliding systems. In this approach, the following set of coupled channel equations [35, 45] is solved numerically.

$$\left[\frac{-\hbar^2}{2\mu}\frac{{\rm d}^2}{{\rm d}r^2}+\frac{J(J+1)\hbar^2}{2\mu r^2}+V_{\rm N}(r)+\frac{Z_{\rm P}Z_{\rm T}e^2}{r}+\varepsilon_n-E_{\rm cm}\right]\psi_n(r)+\sum_m V_{nm}(r)\psi_m(r)=0, \tag{7}$$

where $\boldsymbol{r}$ is the radial coordinate for the relative motion between the fusing nuclei, μ is defined as the reduced mass of the projectile and target system, $E_{\rm cm}$ and ε_n are the bombarding energy in the center of mass frame and the excitation energy of the $n^{\rm th}$ channel respectively,

and $V_{n\,m}$ is the matrix elements of the coupling Hamiltonian, which in the collective model consists of the Coulomb and nuclear components. The coupled channel calculations are performed using the code CCFULL [35] wherein the coupled channel equations are solved numerically. This code includes the couplings to all orders. The set of coupled channel equations are solved using the isocentrifugal approximation and ingoing wave boundary conditions (IWBC). In the isocentrifugal approximation, one can replace the angular momentum of the relative motion of each channel by the total angular momentum. This code also undertakes the finite excitation energy of the intrinsic motion [35, 45]. The ingoing wave boundary conditions (IWBC), which are applicable for heavy ion reactions, are used to obtain the numerical solution of the coupled channel equations [35, 45]. By including the dominant effects of the nuclear structure degrees of freedom, the fusion cross-section can be written as

$$\sigma_{\rm F}(E) = \sum_J \sigma_J(E) = \frac{\pi}{k_0^2} \sum_J (2J+1)\, P_J(E), \qquad (8)$$

where $P_J(E)$ is the total transmission coefficient associated with the angular momentum J.

3 Results and discussion

For ^{90,94}Zr-target isotopes, as they are spherical in shape, the collective surface vibrational states are the dominant mode of couplings. In the case of ^{6}Li + ^{90}Zr and ^{28}Si + ^{90}Zr reactions [30, 36–38], the difference in energy dependence of sub-barrier fusion cross-sections is the signature of dominance of different nuclear structure degrees of freedom of the projectiles, while the difference in the fusion dynamics of ^{28}Si + ^{90,94}Zr reactions mirrors the dominance of different nuclear structure degrees of target isotopes. The values of deformation parameter and the corresponding excitation energy of low lying 2^+ and 3^- vibrational states of fusing nuclei are listed in Table 1. The barrier height, barrier position and barrier curvature of the fusing nuclei used in the EDWSP model calculations are listed in Table 2. In Table 3, the values of potential parameters such as range, depth and diffuseness used in the EDWSP model calculations for the chosen reactions are listed.

Table 1. The deformation parameter (β_λ) and the energy (E_λ) of the quadrupole and octupole vibrational states of various nuclei.

nucleus	β_2	E_2/MeV	β_3	E_3/MeV	Ref.
^{28}Si	0.407	1.780	0.280	6.880	[36]
^{90}Zr	0.090	2.186	0.220	2.748	[34]
^{94}Zr	0.090	0.919	0.200	2.058	[34]

Table 2. The values of $V_{\rm B0}$, $R_{\rm B}$ and $\hbar\omega$ used in the EDWSP model calculations for various heavy ion fusion reactions.

system	$V_{\rm B0}$/MeV	$R_{\rm B}$/fm	$\hbar\omega$/MeV	Ref.
^{6}Li + ^{90}Zr	17.20	9.32	4.22	[30]
^{28}Si + ^{90}Zr	72.06	10.42	3.90	[35]
^{28}Si + ^{94}Zr	71.46	10.52	3.96	[35]

Table 3. Range, depth and diffuseness of the Woods-Saxon potential used in the EDWSP model calculations for various heavy ion fusion reactions [33, 34].

system	r_0/fm	V_0/MeV	$\frac{a^{\rm Present}}{\text{energy range}} \Big/ \frac{\text{fm}}{\text{MeV}}$
^{6}Li + ^{90}Zr	1.070	29.38	$\frac{0.93\,\text{to}\,0.85}{10\,\text{to}\,35}$
^{28}Si + ^{90}Zr	1.080	84.23	$\frac{0.96\,\text{to}\,0.85}{65\,\text{to}\,95}$
^{28}Si + ^{94}Zr	1.100	87.94	$\frac{0.97\,\text{to}\,0.85}{60\,\text{to}\,95}$

The barrier modification effects introduced in the fusion dynamics of ^{6}Li + ^{90}Zr and ^{28}Si + ^{90,94}Zr reactions as a consequence of the energy dependence in the nucleus-nucleus potential are shown in Fig. 1. The static Woods-Saxon potential produces a single Coulomb barrier and therefore, the inclusion of nuclear structure degrees of freedom of the colliding pairs such as inelastic surface excitations, rotational states and nucleon (multi-nucleon) transfer channels are necessarily required in the coupled channel equations to remove the discrepancies between experimental fusion data and the predictions of the one-dimensional barrier penetration model. The additions of the relevant intrinsic channels bring the coupled channel calculations nearer to the experimental data and hence adequately explain the observed sub-barrier fusion enhancement of the various heavy ion fusion reactions. On the other hand, the energy-dependent Woods-Saxon potential modifies the barrier characteristics (barrier height, barrier position, barrier curvature) which in turn generate an energy-dependent fusion barrier of variable height as shown in Fig. 1. In the spectrum of energy-dependent fusion barriers, some barriers are lower than the Coulomb barrier and consequently allow the maximum penetration of the flux from entrance channel to fusion channel. Therefore, the lowering of the effective fusion barrier between colliding systems increases the efficiency of the EDWSP model and hence the present model is capable of predicting larger sub-barrier fusion excitation functions with respect to the expectations of the one-dimensional barrier penetration model. The modification of barrier characteristics (barrier height, barrier position, barrier curvature) is the

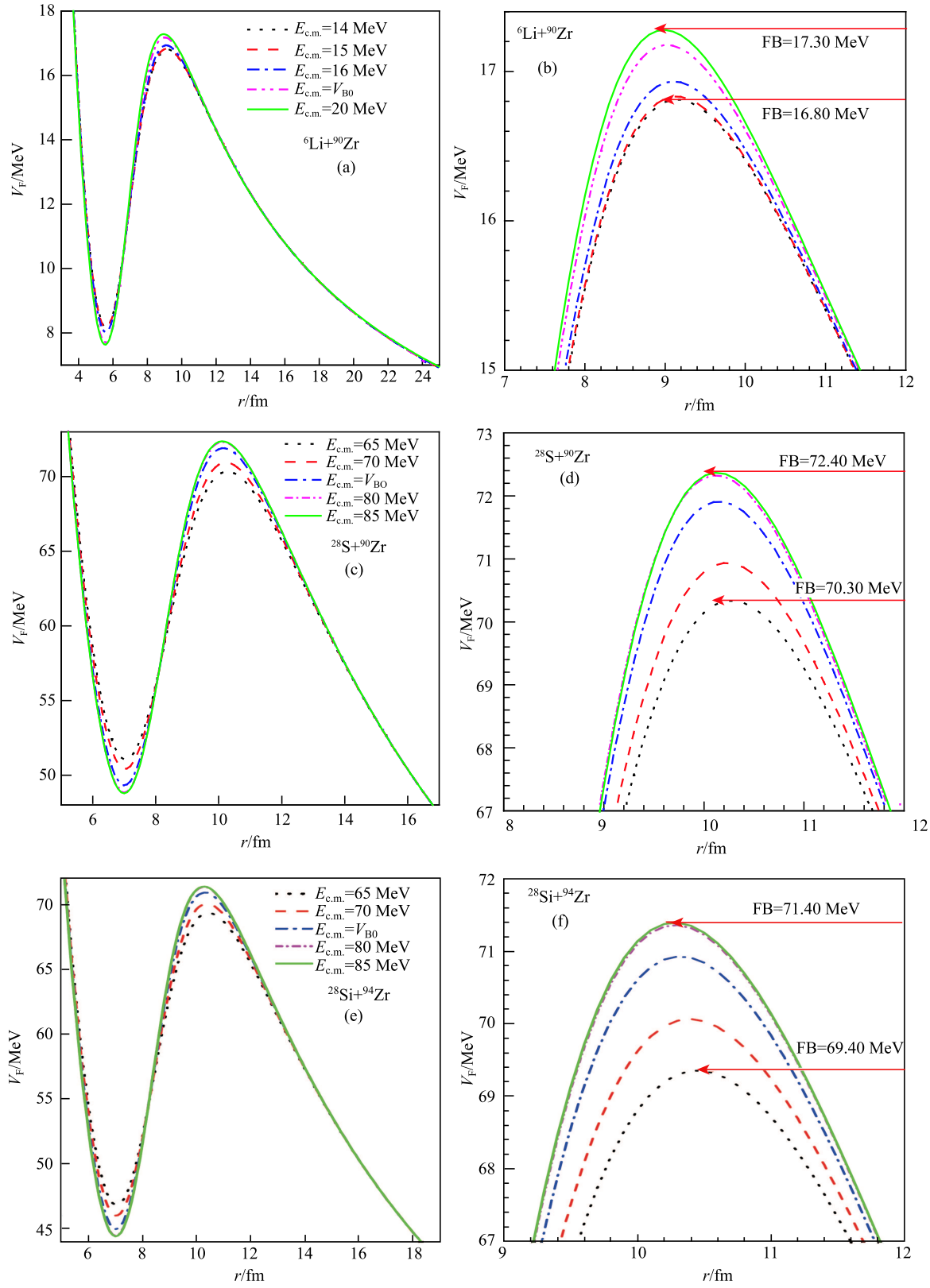

Fig. 1. (color online) The fusion barrier (FB) for ^{6}Li+^{90}Zr and ^{28}Si+^{90,94}Zr systems obtained using the EDWSP model [33, 34].

main ingredient of the EDWSP model and henceforth, adequately explains the observed fusion dynamics of the wide range of projectile-target combinations. The channel coupling effects that arise due to nuclear structure effects like collective surface vibrational states, static deformation, nucleon (multi-nucleon) transfer channels etc. and the barrier modification effects introduced as a consequence of the energy dependence in the Woods-Saxon potential effectively lower the interaction barrier between fusing nuclei and consequently represent similar physical behavior of heavy ion fusion reactions in the domain of the Coulomb barrier.

At deep sub-barrier energies, the longer tail of the fusion barrier of the ^{6}Li+^{90}Zr reaction (see Fig. 1(a, b)) in comparison to that of ^{28}Si+^{90,94}Zr reactions (Fig. 1(c–f)) can be correlated with the loosely bound nature of the projectile. This clearly indicates that the fusion process starts at larger inter-nuclear separation between the colliding systems as compared to the predictions obtained by using the static Woods-Saxon potential. In case of ^{28}Si + ^{90,94}Zr reactions, the longer tail of the fusion barrier of the ^{28}Si+^{94}Zr reaction (Fig. 1(e, f)) relative to the ^{28}Si+^{90}Zr reaction (Fig. 1(c, d)) is a result of the dominance of neutron (multi-neutron) transfer channels in the former system. The inelastic surface excitations of the colliding pairs is the only factor that results in the substantially large sub-barrier fusion excitation functions of the ^{28}Si+^{90}Zr reaction with respect to the expectations of the one-dimensional barrier penetration model, whereas the combined effects of the inelastic surface excitations and multi-neutron transfer channels enhance the magnitude of the sub-barrier fusion excitation function of the ^{28}Si+^{94}Zr reaction with respect to that of the ^{28}Si+^{90}Zr reaction. Therefore, the longer tail of the fusion barrier of ^{28}Si+^{94}Zr reaction relative to ^{28}Si+^{90}Zr reaction physically reveals the dominant effects of neutron (multi-neutron) transfer channels in the former reaction.

In EDWSP model calculations, at below-barrier energies $a = 0.93$ fm is the largest value of the diffuseness parameter for the ^{6}Li+^{90}Zr reaction ($a = 0.97$ fm for the ^{28}Si+^{94}Zr reaction and $a = 0.96$ fm for ^{28}Si+^{90}Zr reaction) that results in the lowest fusion barrier as depicted in Fig. 1. For all three reactions, the lowest fusion barrier produced in the EDWSP model calculation is much smaller than the corresponding value of the Coulomb barrier as listed in Table 2. This supplements the shifting of maximum incoming flux into the fusion channel and consequently results in the larger magnitude of fusion cross-section at below-barrier energies. With increase of incident energy, the value of diffuseness parameter decreases, which in turn increases the height of the corresponding fusion barrier. From theoretical and experimental points of view, it has been recognized that the fusion excitation functions become saturated in the above-barrier energy regions due to the fact that the channel coupling effects have a negligible influence on the above-barrier fusion data [4–6, 30–32]. This physical effect is adequately incorporated in the present model calculations, wherein the variation of diffuseness parameter is saturated to its lowest value in above-barrier energy regions and hence accurately controls the saturation effects of above-barrier fusion excitation function data. The saturation of the diffuseness parameter further limits the fluctuations of the effective fusion barrier between the colliding systems and hence, the invariance (or weak variance) in the height of the fusion barrier at above-barrier energies physically reflects the insensitivity of the fusion excitation functions to various channel coupling effects. Furthermore, the lowest fusion barrier of the ^{28}Si + ^{94}Zr reaction is smaller than that of the ^{28}Si + ^{90}Zr reaction by 0.9 MeV and therefore, predicts larger sub-barrier fusion enhancement for neutron-rich target isotopes. Similar conclusions about the sub-barrier fusion dynamics of ^{28}Si+^{90,94}Zr reactions are also reflected from the coupled channel analysis, wherein the effects of the multi-neutron transfer channels dominate over the inelastic surface excitations in the case of heavier target isotopes.

The detail of coupled channel calculations of the ^{6}Li + ^{90}Zr reaction is shown in Fig. 2. The deformation parameters and the corresponding excitation energies of low lying surface vibrations of the target nucleus are listed in Table 1. The couplings to these inelastic surface excitations of the target isotope are found to play a crucial role in accounting for the sub-barrier fusion data. The ^{6}Li-nucleus is a loosely bound nucleus due to its low breakup threshold and consequently displays the signature of the breakup effects on the fusion excitation functions. If the projectile is taken as an inert nucleus, the inclusion of one phonon 2^{+} and 3^{-} vibrational states along with their mutual coupling with the target isotope produces larger fusion cross-section in comparison to no-coupling calculations. At below-barrier energies, the consideration of single phonon vibrational states of the target nucleus is unable to reproduce the observed fusion dynamics of the ^{6}Li+^{90}Zr system and thus requires further additions of higher vibrational states like two-phonon and three-phonon vibrational states. The coupling strength of the octupole vibrational state is larger than that of the quadrupole vibrational state, therefore the influence of higher order 3^{-} vibrational states on the fusion dynamics of the reaction is more pronounced than other inelastic surface excitations. The inclusion of two-phonon 3^{-} vibrational states along with their mutual couplings with the target isotope improves the theoretical results but still there remains a large discrepancy between the coupled channel calculations and the below-barrier fusion data of the ^{6}Li + ^{90}Zr system. To address this issue, the projectile excitations must be incorporated

in the coupled channel description. The projectile exhibits a non-zero quadrupole moment ($Q_m = -0.082\,\mathrm{fm}^2$) in its ground state and in the unbound first excited state ($3^+, 2.186$ MeV), which must be included in the theoretical analysis. Spectroscopic analysis suggests that the transition probability ($\mathrm{BE2}, 1^+ \to 3^+$) is 21.80 $\mathrm{e}^2\mathrm{fm}^4$ for 3^+ rotational states of the projectile, which lies at the excitation energy of 2.186 MeV. Therefore, when the 3^+ rotational state of the projectile is coupled along with two-phonon vibrational states of the target isotope, we recover the below-barrier fusion data. This clearly indicates that the below-barrier fusion data can only be addressed if one includes the nuclear structure degrees of freedom of the colliding pairs.

However, the inclusion of the projectile excitations in the coupled channel analysis results in suppression of the above-barrier fusion data of the ^{6}Li+^{90}Zr system by 34% with reference to the coupled channel calculations. In Ref. [30–32], the authors performed theoretical calculations of the ^{6}Li+^{90}Zr reaction using the continuum discretized coupled channel (CDCC) approach by treating the projectile as a two-body $\alpha+\mathrm{d}$ cluster structure with a breakup threshold of 1.475 MeV. The dynamic polarization potential produced due to breakup effects is of a repulsive nature in the nuclear surface region for all incident energies, and hence the authors claim that the above-barrier fusion data is suppressed by 34% with respect to the coupled channel calculations. The breakup of the projectile into an α+d cluster structure is also supported by the experimental investigations of Signorini et al. [47]. On the other hand, the EDWSP model calculations provide a complete description of the sub-barrier fusion data but the above-barrier fusion data is also suppressed with respect to the EDWSP model calculations. However, the large discrepancies between coupled channel calculations and the above-barrier fusion data are reduced by 14% as shown in Fig. 2. This suppression of the above-barrier fusion data can be correlated with the breakup of the projectile due to its low binding energy (B.E. = 1.475 MeV). The overestimations of the coupled channel calculations to above-barrier data clearly mirror the loss of flux from the fusion channel to other reaction channels and hence results in the suppression of the fusion excitation functions data with respect to the predictions of the theoretical approaches. The magnitude of the suppression factor is reduced in the EDWSP model calculations by 14% and hence the above-barrier fusion data is suppressed with respect to EDWSP model calculations by 20%, as shown in Fig. 2.

We now consider the fusion dynamics of the ^{28}Si+^{90,94}Zr reactions, where colliding nuclei are stable against breakup effects. The consideration of fusion dynamics of these reactions includes (i) extracting an unambiguous statement with regard to the projectile breakup effects, and (ii) disentangling the impact of the neutron (multi-neutron) transfer channel on the inelastic surface vibrational states of the colliding pairs. Due to the stability of the projectile against the breakup channel, the above-barrier fusion data is not suppressed with respect to the theoretical predictions and hence is adequately explained by the theoretical calculations due to the EDWSP model and coupled channel approach as evident from Figs. 3, 4.

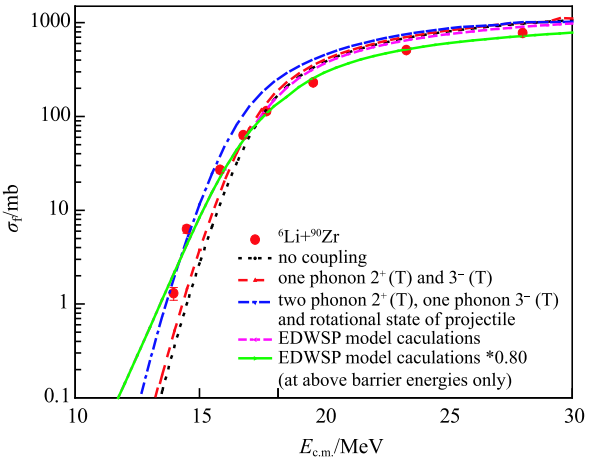

Fig. 2. (color online) The fusion excitation functions of the ^{6}Li+^{90}Zr reaction are obtained using the EDWSP model [33, 34] and the coupled channel code CCFULL [35]. The results are compared with available experimental data taken from Ref. [30].

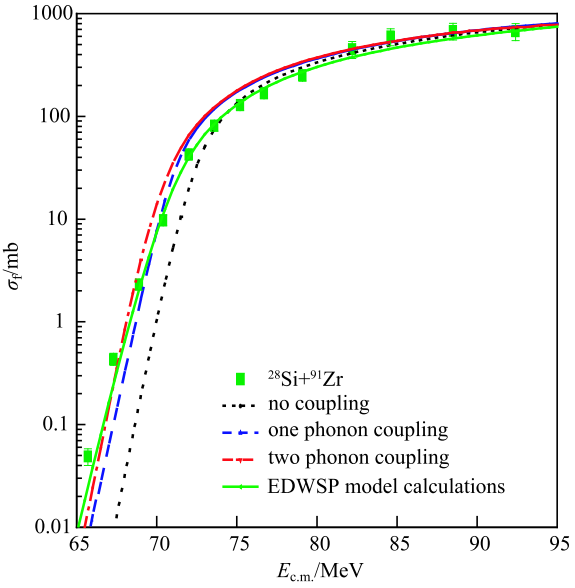

Fig. 3. (color online) The fusion excitation functions of ^{28}Si + ^{90}Zr reaction obtained using the EDWSP model [33, 34] and the coupled channel code CCFULL [35]. The results are compared with available experimental data taken from Ref. [36].

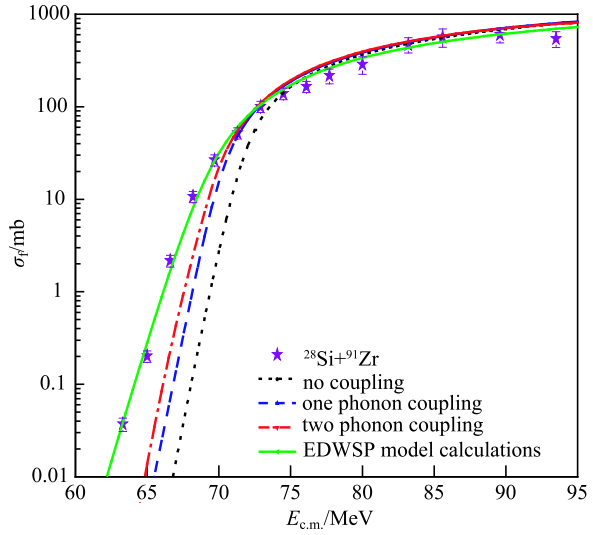

Fig. 4. (color online) The fusion excitation functions of ^{28}Si + ^{94}Zr reaction obtained using the EDWSP model [33, 34] and the coupled channel code CCFULL [35]. The results are compared with available experimental data taken from Ref. [36].

In the case of the ^{28}Si+^{90}Zr reaction, the colliding nuclei are dominated by inelastic surface excitations like 2^+ and 3^- vibrational states. The coupling to these nuclear structure degrees of freedom of the colliding pairs results in the substantially larger sub-barrier fusion enhancement over the expectations from the one-dimensional barrier penetration model. The no-coupling calculations, wherein colliding pairs are treated as inert, are significantly smaller than those of the experimental fusion data at below-barrier energies, while the above-barrier data have been properly recovered. The coupling to one-phonon vibrational states such as 2^+ and 3^- vibrational states of the target and the single-phonon 2^+ and 3^- vibrational states of the projectile significantly improve the results. There remain large deviations, however, between the coupled channel calculations and below-barrier fusion data. This demands the addition of the more intrinsic channels in the coupled channel calculations for addressing the sub-barrier fusion enhancement. Therefore, the inclusion of one-phonon 2^+, two-phonon 3^- vibrational states of the target and one-phonon 2^+ and 3^- vibrational states of the projectile, along with their mutual couplings, reasonably explain the observed fusion dynamics of the ^{28}Si + ^{90}Zr reaction. In this case, the transfer channels do not have a significant contribution to the enhancement of the fusion excitation function due to fact that the nucleon (multi-nucleon) transfer channels have negative ground state Q-values. The α- pickup channel has a small positive ground Q-value ($Q = +0.28$ MeV), but in Refs. [36–38] it is clearly shown that the magnitude of sub-barrier fusion enhancement is insensitive to the addition of such channels. Therefore, the existence of fewer neutron transfer channels with very small transfer probability is due to neutron shell closure of the target isotope. In contrast to this, the barrier modification effects (see Fig. 1(c, d)) introduced in the EDWSP model calculations lower the effective fusion barrier between the colliding systems and hence provide a complete description of the fusion dynamics of the ^{28}Si+^{90}Zr reaction. Therefore, the observed sub-barrier fusion enhancement of the ^{28}Si + ^{90}Zr reaction occurs due to the dominant effects of the inelastic surface excitations of the colliding pairs and such nuclear structure effects are adequately simulated in the present model calculations as evident from Fig. 3.

The same coupling scheme as used for the ^{28}Si + ^{90}Zr system has been tested to explain the fusion dynamics of ^{28}Si + ^{94}Zr reaction, but such a coupling scheme fails to recover the observed fusion enhancement of the neutron-rich target isotope, as shown in Fig. 4. The inclusions of one-phonon 2^+ and 3^- vibrational states along with their mutual couplings bring the sub-barrier fusion enhancement with respect to the no-coupling calculations but cannot address the below-barrier fusion data. The significantly large deviations between the coupled channel calculations and the below-barrier fusion data demand the addition of more intrinsic channels in order to recover the sub-barrier fusion enhancement. The couplings to one-phonon 2^+ and two-phonon 3^- vibrational states along with their mutual couplings in the target and the single-phonon 2^+ and 3^- vibrational states of the projectile, along with their mutual couplings, significantly improve the theoretical results. However, such calculations are unable to address the below-barrier fusion enhancement. The fusion dynamics of the ^{28}Si + ^{94}Zr system facilitates the possibility of the transfer of 4-neutrons with positive ground state Q-values. In addition to this, one proton stripping channel also exists but the probability of transferring four neutrons is quite large in comparison to that of the proton transfer channel. The discrepancies between the coupled channel calculations and experimental data, particularly at below-barrier energies, can be correlated with these neutron transfer channels. The authors in Ref. [36] explicitly shown that in addition to inelastic surface excitations of the colliding pairs, the couplings to neutron transfer channels are required in order to account for the sub-barrier fusion enhancement. The additional neutron tries to deform the shape of the nucleus during collision and thus is responsible for a decrease in the height of the Coulomb barrier, resulting in greater penetration probability. In Ref. [36], the role of the multi-nucleon transfer couplings was found to increase as one moves from the lighter target isotope (^{90}Zr) to the heavier target isotope (^{94}Zr). Very recently the coupled channel analysis of the ^{28}Si + ^{94}Zr system

has shown that the effects of one- and two-proton stripping also play an important role at energies well above the barrier. In the EDWSP model calculations, the barrier lowering effects originate as a consequence of the energy-dependence in the nucleus-nucleus potential and predict significantly larger sub-barrier fusion excitation functions with reference to the expectations of the single barrier penetration model calculations. Hence, it reasonably explains the observed fusion dynamics of the ^{28}Si + ^{94}Zr system in the whole range of energy spread across the Coulomb barrier, as evident from Fig. 4. Furthermore, the larger sub-barrier fusion enhancement of the ^{28}Si+^{94}Zr system arises due to the combined effects of inelastic surface excitations and neutron (multi-neutron) transfer channels, and such physical effects are properly incorporated in the energy-dependent nucleus-nucleus potential.

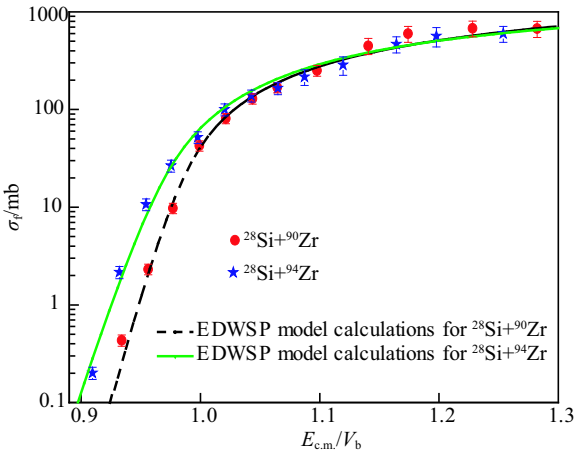

Fig. 5. (color online) The fusion excitation function data of the ^{28}Si + ^{90,94}Zr reactions [36] along with theoretical results obtained using the EDWSP model [33, 34].

In the fusion of ^{28}Si + ^{90,94}Zr reactions, the projectile is common to the ^{90,94}Zr-target isotopes; therefore different features of these reactions are the result of different nuclear structure of the target isotopes. The lighter target rules out the possibility of the multi-neutron transfer channels while the heaver target allows the multi-neutron transfer channels with positive ground state Q-values. Therefore, the larger sub-barrier fusion enhancement of the ^{28}Si+^{94}Zr system with respect to the ^{28}Si+^{90}Zr system is the result of neutron transfer between the colliding pairs, as depicted in Fig. 5. As already mentioned, similar conclusions with regard to the fusion dynamics of ^{28}Si+^{90,94}Zr reactions are also reflected from the EDWSP model calculations. In short, the observed sub-barrier fusion enhancement of ^{6}Li+^{90}Zr and ^{28}Si+^{90,94}Zr reactions arises due to the involvement of nuclear structure degrees of freedom like collective surface vibrational states, rotational states and nucleon (multi-nucleon) transfer channels. However, the suppression of the above-barrier fusion data of the ^{6}Li + ^{90}Zr reaction is the consequence of projectile breakup effects that occur due to its low breakup threshold. Such suppression effects are absent in the above barrier energy region of the ^{28}Si + ^{90,94}Zr reactions and hence confirms the stability of the ^{28}Si-isotope against breakup effects.

4 Conclusions

This work analyzed the fusion dynamics of ^{6}Li+^{90}Zr and ^{28}Si+^{90,94}Zr reactions within the context of the coupled channel approach and the EDWSP model. In the fusion of ^{28}Si + ^{90}Zr reaction, the couplings to inelastic surface excitations are found to be the dominant mode of coupling whereas in the fusion of the ^{28}Si+^{94}Zr reaction, the inclusions of collective surface vibrational states of colliding systems as well as the neutron transfer channels are required to account for the observed fusion dynamics. The larger sub-barrier fusion enhancement of ^{28}Si + ^{94}Zr reaction with reference to ^{28}Si + ^{90}Zr reaction can be correlated with the large probability of neutron (multi-neutron) transfer channels with positive ground state Q-values in the former system, while such characteristics are absent in the latter system. On the other hand, the EDWSP model calculations induce barrier modification effects (barrier height, barrier position, barrier curvature) which in turn effectively lower the fusion barrier between the colliding systems and consequently explain the observed fusion dynamics of the ^{28}Si + ^{90,94}Zr reactions. In both reactions, there is no signature of suppression of the above barrier fusion data, which confirms the stability of the projectile (^{28}Si) against breakup effects.

In contrast to this, the above-barrier fusion data of the ^{6}Li + ^{90}Zr reaction is suppressed with respect to the predictions of both theoretical approaches (coupled channel approach and EDWSP model). Interestingly, in the EDWSP model calculations, the suppression of the above-barrier fusion data is reduced by 14%. Therefore, the above-barrier fusion data of the ^{6}Li + ^{90}Zr reaction is suppressed by 20% with respect to the EDWSP model calculations, which is much smaller than the 34% reported in the literature. The projectile (^{6}Li) is a loosely bound nucleus due to its low breakup threshold. The projectile breaks up in the entrance channel before reaching the fusion barrier, which decreases the incoming flux going into the fusion channel and hence automatically regulates the suppression of fusion data in above-barrier energy regions. At below-barrier energies, fusion enhancement of the ^{6}Li+^{90}Zr reaction occurs due to involvement of the nuclear structure degrees of freedom of the colliding systems, and hence is adequately addressed by both theoretical approaches (coupled channel approach and EDWSP model).

References

1 C. Beck et al, Phys. Rev. C, **67**: 054602 (2003)
2 C. Beck, Journal of Physics: Confernece Series, **420**: 012067 (2013)
3 M. S. Gautam, Phys. Scr., **90**: 025301 (2015)
4 J. R. Bierman et al, Phys. Rev. Lett., **76**: 1587 (1996)
5 L. F. Canto et al, Phys. Rep., **424**: 1 (2006)
6 B. B. Back et al, Rev. Mod. Phys., **86**: 317 (2014)
7 M. S. Gautam, Nucl. Phys. A, **933**: 272 (2015)
8 L. T. Baby et al, Phys. Rev. C, **62**: 014603 (2000)
9 A. A. Sonzogni et al, Phys. Rev. C, **57**: 722 (1998)
10 A. M. Vinodkumar et al, Phys. Rev. C, **53**: 803 (1996)
11 N. V. S. V. Prasad et al, Nucl. Phys. A, **603**: 176 (1996)
12 A M Stefanini et al, Phys. Lett. B, **728**: 639 (2014)
13 M. S. Gautam, Phys. Scr., **90**: 055301 (2015), Phys. Scr., **90**: 125301 (2015)
14 Y. W. Wu et al, Phys. Rev. C, **68**: 044605 (2003)
15 Z.H. Liu et al, Eur. Phys. J. A, **26**: 73 (2005)
16 M. S. Hussein et al, Phys. Rev. C, **46**: 377 (1992)
17 M. S. Hussein et al, Phys. Rev. C, **51**: 846 (1995)
18 M. S. Gautam, Can. J. Phys., **93**: 1343 (2015); Chinese Phys. C, **39**: 114102 (2015); Indiam J. Phys., **90**: 335 (2016); Braz. J. Phys., **46**: 143 (216)
19 C. H. Dasso et al, Phys. Rev. C, **50**: (1994) R12
20 C. H. Dasso et al, Phys. Lett. B, **276**: 1 (1992)
21 K. E. Zyromski et al, Phys. Rev. C, **55**: R562 (1997)
22 P. A. DeYong et al, Phys. Rev. C, **58**: 3442 (1998)
23 J. J. Kolata et al, Phys. Rev. Lett., **81**: 4580 (1998)
24 M. Trotta et al, Phys. Rev. Lett., **84**: 2342 (2000)
25 M. Dasgupta et al, Phys. Rev. Lett., **82**: 1395 (1999)
26 C. Signorini et al, Eur. Phys. J. A, **5**: 7 (1999)
27 M. Dasgupta et al, Phys. Rev. C, **66**: 041602(R) (2002)
28 P. K. Rath et al, Phys. Rev. C, **79**: 051601 (2009)
29 V. Tripathi et al, Phys. Rev. Lett., **88**: 172701 (2002)
30 H. Kumawat et al., Phys. Rev. C, **86**: 024607 (2012)
31 I. J. Thompson, Com. Phys. Report, **7**: 167 (1988)
32 A. Diaz-Torres and I. J. Thompson, Phys. Rev. C, **65**: 024606 (2002)
33 M. Singh, Sukhvinder and R. Kharab, Nucl. Phys. A, **897**: 179 (2013); Nucl. Phys. A, **897**: 198 (2013); Mod. Phys. Lett. A, **26**: 2129 (2011)
34 M. S. Gautam, Phys. Rev. C, **90**: 024620 (2014); M. S. Gautam et al, Phys. Rev. C, **92**: 054605 (2015); Braz. J. Phys. **46**: 133 (2016)
35 K. Hagino, N. Rowley and A. T. Kruppa, Comput. Phys. Commun, **123**: 143 (1999)
36 S. Kalkal et al, Phys. Rev. C, **81**: 044610 (2010)
37 S. Kalkal et al, Phys. Rev. C, **83**: 054607 (2011)
38 S. Kalkal et al, Phys. Rev. C, **85**: 034606 (2012)
39 M. S. Gautam, Mod. Phys. Lett. A, **30**: 1550013 (2015)
40 M. S. Gautam, Acta. Phys. Pol. B, **46**: 1055 (2015)
41 C. Y. Wong, Phys. Rev. Lett., **31**: 766 (1973)
42 D. L. Hill and J. A. Wheeler, Phys. Rev., **89**: 1102 (1953)
43 L. C. Chamon et al., Phys. Rev. C, **66**: 014610 (2002)
44 K. Washiyama and D. Lacroix, Phys. Rev. C, **74**: 024610 (2008)
45 K. Hagino and N. Takigawa, Prog. Theor. Phys., **128**: 1061 (2012)
46 E. F. Aguilera and J. J. Kolata, Phys. Rev. C, **85**: 014603 (2012)
47 C. Signorini et al, Phys. Rev. C, **67**: 044607 (2003)